

# The Analysis of the Influence of Technological Parameters on the Grinding Temperature in the Single-Pass Grinding Process of Solid Carbide End Mill Flutes

Marcin Sałata<sup>1</sup>

<sup>1</sup> Faculty of Mechanical Engineering and Aeronautics, Rzeszów University of Technology, al. Powstańców Warszawy 12, 35-959 Rzeszów, Poland  
e-mail: msalata@prz.edu.pl

## ABSTRACT

A method of the measurement of temperature and grinding force components during flute grinding of solid carbide end mills was presented. The tests were performed using two diamond grinding wheels: with a resin bond (S1) and with a metal bond (S2). A diamond grinding wheel of 1A1 type and a rectangular cross-section was used. An ultrafine grained carbide with a grain size of 0.2 to 0.5  $\mu\text{m}$ , characterized by high hardness (1730 HV30) and very high tensile strength (4600 MPa) was used. The flutes were grinded in one pass, thus replacing roughing and finishing. The temperature of grinding was recorded using thermocouple type K, NiCr-Ni. The measurement of forces was conducted using a rotary piezoelectric dynamometer. Surface topography was recorded with the Alicona InfiniteFocus G4 microscope. The experiment was planned in Design-Expert 13 software. Mathematical models were developed, describing the relationships between the grinding speed and the feed rate as a function of the grinding temperature, grinding force and roughness parameters of the flute. For both grinding wheels, the  $F_n$  grinding force was recorded in the range of 28–110 N, the temperature in the range of 32–200 °C and surface roughness  $S_a$  in the range of 0.31–0.76  $\mu\text{m}$ . The best grinding result, in terms of low grinding forces and temperatures was achieved for the grinding wheel with the metal bond (S2). For the resin grinding wheel (S1), for the selected technological parameters, grinding burn occurred.

**Keywords:** grinding temperature, single-pass grinding, flute grinding.

## INTRODUCTION

The main issue of the currently manufactured solid carbide end mills is the production time and the complexity of the tool design as discussed by Malkin [1], Hubert [2] and also Fujara [3]. The basic operation in the manufacturing of carbide tools is the flute grinding process, presented by Christoph [4] as well as Guachao [5]. It takes up to 70% of the production time, which was proved in works presented by Burek [6, 7]. Machining of the flute takes place in many stages, and the roughing and finishing require from a few to a dozen grinding wheel passes, which significantly extends the grinding time as discussed by Yang [8]. The method of deep grinding, which is constantly the subject of research, consists of

removing the entire machining allowance in a single pass of a grinding wheel, thus replacing the multi-stage roughing and finishing presented by Uhlmann [9] and also Badger [10]. Therefore, the optimization of technological parameters ( $v_s$ ,  $v_f$ ) is of great importance which was proved in works presented by Bazan [11, 12].

Among the many grinding parameters, in the monitoring systems used so far, the most common monitoring parameter has been the grinding force, because its variations very well correspond with the characteristics of the process which was also discussed in the work by Ren [13]. Grinding temperature is another parameter allowing to monitor the machining as discussed by Shatov [14] and Sui [15]. High temperatures, especially in single-pass grinding can lead to damage of the grinded end

mills as well as diamond grinding wheels, which was proved in works presented by Ren [16] and Yang [17]. In addition, due to thermal expansion, the dimension of the workpiece may change, which may result in shape and dimensional errors presented by Bazan [18]. Thus, thermal analysis of the grinding process is so important, which was proved in works presented by Grochalski [19].

Ren et al. [20] describes a method (an algorithm) of five-axis flute grinding using standard 1V1/1A1 grinding wheels. Adopting the algorithm allows for precise calculation of the grinding wheel's position in terms of the three most important parameters defining the flute (rake angle, core radius and flute width). The experimental tests described in the following paper adopted a standard algorithm of calculating the flute geometry available in the CNC machine tool control. Abdullah et al. [21] in their paper describe the diamond grinding wheel wear process during single-pass deep grinding, also called creep-feed grinding. Analyzing the results of their work, one can observe that technological parameters influence wear of the diamond grinding wheels. In the following paper grinding wheel wear was considered negligible, due to the short length of the grinded flute. Habrat et al. [22] in their work describe the influence of diamond wheel's bond on the grinding force components during carbide grinding. The obtained results indicate that the grinding speed, feed rate and grinding depth influence tangential and normal grinding force components. Grochalski et al. [23] in their work present two methods of temperature measurement: with the use of a thermal imaging camera and with a thermocouple. For the most resistant to measuring problems method authors indicate measurement with a thermocouple. Such a method was implemented in the following paper.

Regardless of the direction of the studies, researches emphasize the fact that machining of carbide, which is one of the difficult-to-cut materials, remains a constant challenge in terms of machining efficiency. It is especially important when considering new carbide types, such as ultrafine grade carbide or new diamond wheels with hybrid bond. It should also be noted that in solid end mills, flute is a critical part that determines parameters such as rake angle, core radius and flute width. These three parameters significantly influence grinding force, temperature, chip removal efficiency and tool life. Thus, ensuring their accuracy during machining and their continuous monitoring is of utmost importance.

The paper presents the attempt of using the K type thermocouple (NiCr-Ni) to measure the temperature of solid carbide end mill flutes during single-pass grinding with diamond grinding wheels.

## EXPERIMENTAL RESEARCHES

Equipped with ISOG CNC FORTIS grinding machine test stand, researches of grinding process of flute in solid carbide end mill were performed (Fig. 1). The machine is a 5-axis grinding centre with three linear axes (X, Y, Z) and two rotary axes (A, C), spindle power 6 kW, spindle speed from 1000 to 8000 rpm. During the measurement of grinding forces KISTLER rotary dynamometer type 9123 was used. It is multi-channel, piezoelectric, adapted to measure three grinding forces components as well as torque ( $M_c$ ) in two measurement ranges. To make the measurement even more accurate and to minimize measuring noise, the accuracy of measurement increased through measuring in second range which amounts to  $F_x = 0-450$  N,  $F_y = 0-450$  N,  $F_z = 0-1800$  N.

In the measuring scheme measured values of cutting force components are converted in dynamometer's 12-bit A/C converter into digital value. Next they are transmitted wirelessly to nonrotating parts of the dynamometer. Then the signal is sent to amplifier, type 5223B. In the amplifier the signal is again changed into analog. Measurement frequency bandwidth of the device is in the range from 0 to 1 kHz. These signals are then transmitted to the National Instruments A/C NI USB-6009 converter (14 bit, +/-10 V) working under control of the LabVIEW SignalExpress software, which registers test signals. It was registered with 5 kHz rate and 250 samples, which enables to achieve proper resolution allowing to measure grinding forces components [24].

Surface topography studies were carried out using Focus Variation (FV) microscope Alicona InfiniteFocus G4 (Fig. 2).

Processing of the measurement data together with the calculation of 3D parameters of the geometric structure of the surface was carried out in SPIP 6.4.2 software. Data processing included removal of unusually high peaks and deep cavities resulting from coarse measurement errors and filtering of the shape profile with a polynomial of the first degree. 2D and 3D images of the topography maps of

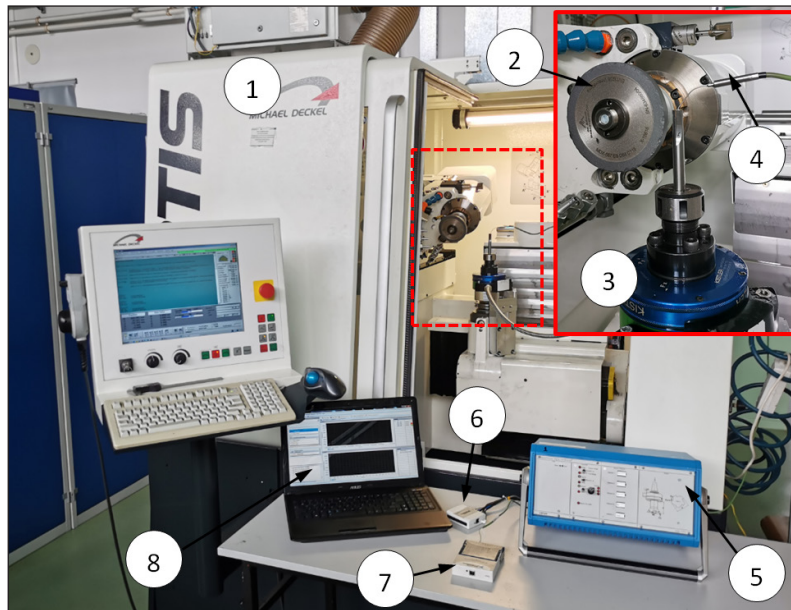


**Fig. 1.** Stand for testing the flute grinding process: 1- five axes grinding center, 2- diamond wheel, 3- KISTLER rotary dynamometer type 9123, 4- NiCrNi thermocouple, 5- Kistler amplifier type 5223B, 6- A/C NI USB converter type 6009, 7- A/C NI converter type 9211, 8- computer

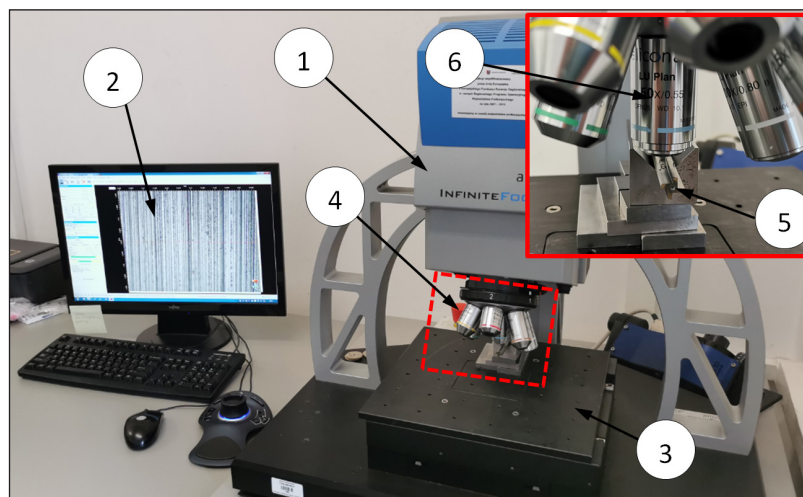


**Fig. 2.** Test stand for measuring 2D, 3D surface topography: 1- Focus Variation microscope Alicona InfiniteFocus, 2- view of measured surface topography, 3- table, 4- objectives, 5- measured sample, 6- objective with x50 magnification

the original profile of the measured surfaces were produced [25]. 3D parameters such as  $S_a$ ,  $S_z$  were calculated. An x50 objective was used for the study. More measurement conditions are shown in Table 1.

**Table 1.** Measurement conditions

Objective	x50
Vertical resolution	50 nm
Lateral resolution	2.13 $\mu\text{m}$
Pixel size	176 nm x 176 nm
Measured area	1.04 mm x 0.22 mm

The Alicona InfiniteFocus microscope uses a measurement method called Focus Variation (FV). FV is a surface-based method in which multiple points are measured during a single scan. FV microscopes use the image sharpness information of the measured surface to determine its height as a function of the z position (x,y), which is made possible by combining the small depth of field of the optical system with vertical scanning. The operating principle is that the optical system is moved vertically along the optical axis to the extent that all points of the surface to be measured are in focus. At certain

positions within the given range, white light is emitted, which passes through the optical system and is focused on the measured surface. All rays reflected from the surface that returns to the objective lens end up on the detector. Due to the small depth of field of the optical system, only a small area of the measured surface is in focus for each position, allowing the vertical position of the optical system to be associated with high information from the measured surface. For each measured point, the actual color information is obtained, allowing photos of the surfaces to be taken.

### MEASUREMENT OF GRINDING TEMPERATURE

In the article the method of temperature measurement during flute grinding was proposed. The method is easy to apply, fast as well as it offers the ability to measure and acquire the results online without stopping the machining. It is a contact method which uses a calibrated thermocouple. Its usage is connected with many advantages comparing to different kinds of temperature sensors. For example: it doesn't require external power supply, small size, low heat capacity, low response time, simple design as well as high reliability. Thermocouple is an element of electric circuit consisting of two different metal made wires. The place of their connection is called a measuring joint, remaining ends are called "cold ends". In that thermocouple electromotive force occurs in case when measuring joint and cold ends are kept in different temperatures (Fig. 3). The thermocouple uses the Seebeck effect, which was discovered in 1821 by German physicist Thomas Johann Seebeck. The reference point of a thermocouple is located in a converter. Temperature of surrounding indicated there is registered in constant way and included in the calculations.

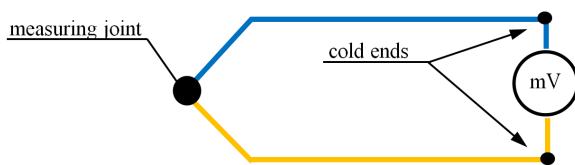


Fig. 3. Scheme of the thermocouple connection with one joint

The temperature of grinding was recorded using thermocouple type K, NiCr-Ni class I coupled with National Instruments A/C NI 9211 converter working under supervision of LabVIEW SignalExpress software which registers test signal on the computer.

One of disadvantages of using a thermocouple is that output voltage equals a few microvolts per degree Celsius. That fact forces to apply A/C card with much higher measure resolution than the one that has been used to measure grinding force component. The input range affects the resolution of the USB-6009 device (for measurement of cutting forces) for an AI channel. For example, a 14-bit ADC converts analog inputs into one of 16 384 ( $= 2^{14}$ ) codes—that is, one of 65 536 possible digital values [26]. So, for an input range of  $-10\text{ V}$  to  $10\text{ V}$ , the voltage of each code of a 14-bit ADC is:

$$\frac{(10V - (-10V))}{2^{14}} = 1220\ \mu V \quad (1)$$

Due to too low card resolution, Ni 9211, (24 bit +/- 80 mV) measure card was used. So, for an input range of  $-80\text{ mV}$  to  $80\text{ mV}$ , the voltage of each code of a 24-bit ADC is:

$$\frac{(0.08V - (-0.08V))}{2^{24}} = 0.0095\ \mu V \quad (2)$$

Card resolution of approximately  $0.009\ \mu V$  was obtained, which is enough to measure the temperature where the thermocouple sensitivity equals  $40\ \mu V/^{\circ}C$  [27].

Inserting measuring probes as close as possible to the machining zone was a problem during contact measurement. For this purpose a hole was made in the blank's axis and consequently the thermocouple was put in there. The hole was made in the process of EDM (electrical discharge machining) on the AccuteX AH-35ZA device using copper electrode of a 1.4 mm diameter (Fig. 4).

For the purpose of ensuring good thermal conductivity – space between the material and the thermocouple was filled with some thermal compound [19]. This procedure prevented the coolant getting into the eroded hole. In order to ensure repeatability of experimental tests, the eroded holes were subjected to the measurements of the diameter, out-of-roundness and concentricity. The eroded holes with the highest deviations were rejected. The hole and its setting is shown in Figure 5. In Table 2 the accuracy of eroded hole is shown.



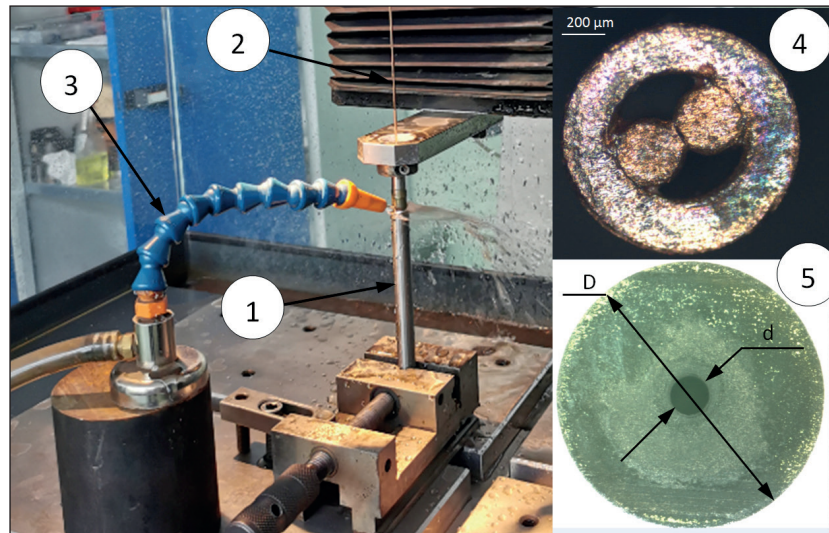


Fig. 4. Stand test for EDM drilling: 1- end mill blank, 2- copper electrode, 3- coolant, 4- electrode top view, 5- eroded hole view, D- blank diameter, d- diameter of eroded hole

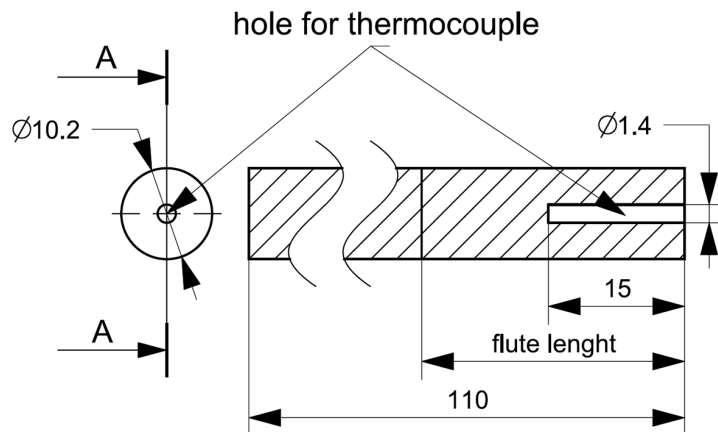


Fig. 5. The eroded hole and its setting

Table 2. Shape and position deviations of the eroded holes

No.	Diameter eroded hole d, mm	Out-of-roundness, mm	Concentricity, mm
1	1.510	0.044	0.027
2	1.512	0.038	0.025
3	1.508	0.043	0.029
4	1.509	0.040	0.022
5	1.510	0.042	0.023
6	1.511	0.039	0.024

- S2: 1A1 D100 U10 X10 H20 D64 C115 – metal bond

The difference between those diamond wheels is their bond. These are:

- 1A1 wheels with a rectangular cross – section,
- nominal diameter of 100 mm, 10 mm width,
- with an average size of a diamond grain of 64 μm in diameter,
- with C115 grain concentration which is 28.75% of the diamond volume in the entire abrasive layer.

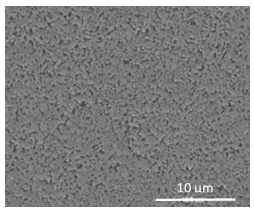
Carbide type TSF44, 10.2 mm in diameter was grinded during the tests. Its features are shown in Table 3. This type of carbide is classified as ultrafine grade and is characterized by the highest transverse rupture strength available on the market (4600 MPa), with maintaining high hardness (1730 HV30). Ultrafine carbide grade for HSC

## MATERIALS AND METHODS

For single – pass grinding process of flute two diamond wheels were used:

- S1: 1A1 D100 U10 X10 H20 D64 C115 – resin bond

**Table 3.** Properties of grinded carbide

Grade	Classification	Grain size	Co	WC	Density	Hardness	Transverse rupture strenght	Structure
TSF44	Ultrafine grades	[ $\mu\text{m}$ ]	%	%	$\text{g/cm}^3$	HV30	MPa	
		0.2 – 0.5	12	88	14.1	1730	4600	

machining (high speed cutting) of tempered steels up to 60 HRC is suitable for micro-tools and finishing tools and for a variety of materials.

In the experiment the variables were the two parameters of the grinding process:

- Grinding speed  $v_s = 15 \div 25$  m/s;
- Feed rate  $v_f = 10 \div 30$  mm/min.

The constant parameters of the grinding process were respectively: grinding width  $a_e = 3$  mm, grinding depth  $a_p = 4.64$  mm, diameter of blank  $D = 10.2$  mm, number of flutes  $z = 4$ , grinding length  $L = 30$  mm, cross-section area of the cutting layer

$A = 10.02$  mm<sup>2</sup>. The blanks was climb grinded. Flood cooling was applied with the usage of “Sin-toGrind” oil. For simplicity straight flutes were cut as shown in Figure 6.

The experiment (DoE) was planned in Design-Expert 13 software. One of the methods used in designing of experiments is the surface response method (RSM) – multicomponent research designs are based on it [28]. For the researches central composite face centered design (CCF) was applied for two dependent variables assuming levels of values ( $3^2$ ) where  $\alpha = 1$ . Graphic interpretation of this plan was shown in Figure 7 [29, 30].

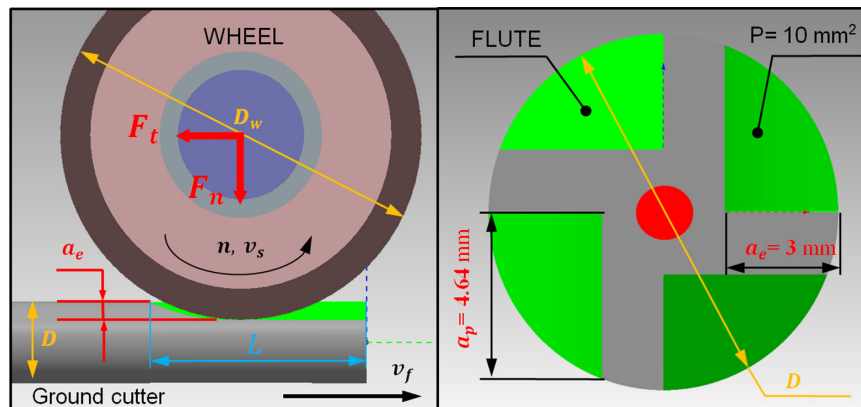


**Fig. 6.** Kinematics of five-axis, single pass flute grinding:  $F_t$  – tangential component of the grinding force,  $F_n$  – normal component of the grinding force,  $D_w$  – grinding wheel diameter,  $v_s$  – cutting speed,  $v_f$  – feed rate,  $D$  – blank diameter,  $L$  – grinding length,  $a_p$  – grinding depth,  $a_e$  – grinding width,  $P$  – cut layer cross-section area

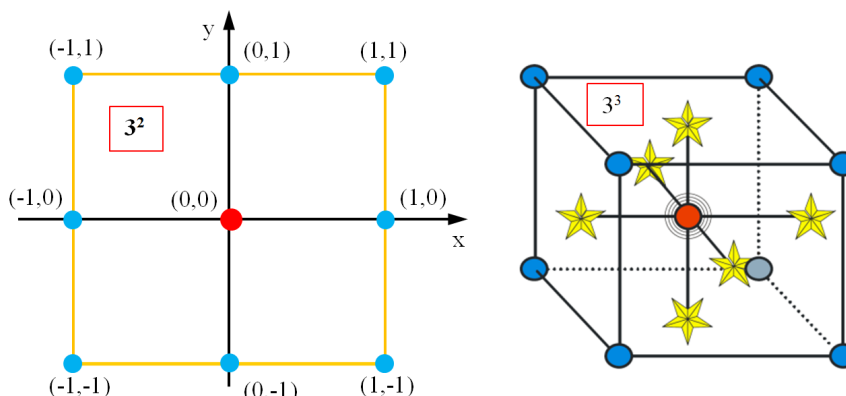


**Fig. 7.** Graphic interpretation of the CCF plan

This experiment is characterized by the fact, that each factor has only three levels. It was used due to the fact that region of interest and region of operability are almost the same. It is characterized by good design properties for designs up to 5 factors, little collinearity, cuboidal rather than rotatable, insensitive to outliers and missing data. It is not recommended for six or more factors due to high collinearity in squared terms [31]. A modified polynomial models was selected for fitting, containing only statistically significant elements. The

significance of the influence of individual input parameters and their interactions was determined based on the ANOVA analysis of variance. Statistical significance of the effect was demonstrated for an assumed confidence level of 95%.

Models obtained by this method can be the basis for optimizing process inputs due to the adopted objective function [32]. The experiment was carried out according to appropriate sets of process input parameters values generated using the Design-Expert software (Table 4).

**Table 4.** List of input parameters, measured values and calculated values

No.	Parameter				S1- Resin bond			S2 – Metal bond		
	$v_s$	$v_f$	$Q_w$	$Q'_w$	$T$	$F_n$	Sa	$T$	$F_n$	Sa
	m/s	mm/min	mm <sup>3</sup> /min	mm <sup>3</sup> /mm·min	°C	N	µm	°C	N	µm
1	15	30	301	65	170.0	110.0	0.449	105.0	90.01	0.713
2	25	20	201	43	117.4	47.04	0.447	45.9	28.60	0.684
3	25	30	301	65	199.4	81.14	0.490	73.7	49.77	0.670
4	15	10	100	22	68.1	37.43	0.317	32.7	29.92	0.692
5	20	10	100	22	74.1	38.41	0.310	40.3	33.77	0.731
6	15	20	201	43	149.2	92.04	0.366	73.4	80.43	0.625
7	20	30	301	65	189.9	94.1	0.445	97.2	80.25	0.660
8	20	20	201	43	133.9	62.3	0.392	60.1	47.08	0.656
9	20	20	201	43	134.0	65.34	0.380	64.0	49.01	0.764
10	25	10	100	22	92.0	40.33	0.420	45.1	33.35	0.583

## RESULTS AND ANALYSIS

According to the assumed research parameters, the performance indicators were calculated as follows:

- grinding efficiency:

$$Q_w = A * v_f \left[ \frac{mm^3}{min} \right] \quad (3)$$

where:  $A$  – is the cross-sectional area of the flute, mm<sup>2</sup>,  $v_f$  – is the feed rate, mm/min.

- specific grinding efficiency:

$$Q'_w = \frac{Q_w}{b_s} \left[ \frac{mm^3}{min * mm} \right] \quad (4)$$

where:  $b_s = a_p$  – is the active grinding wheel width, mm.

After the tests had been carried out, the values of  $F_n$  grinding force, temperature  $T$  and surface roughness  $Sa$  (arithmetical mean height of a surface),  $Sz$  (the greatest height of the surface)

were analyzed. For the fitting, a modified square model was selected. It contained only statistically significant elements ( $\alpha < 0.1$ ). The goodness of fit for the obtained models was determined based on:

- standard deviation of the residua component  $s$ ,
- mean value  $y$ ,
- coefficient of variation C.V., %
- determination coefficients  $R^2$ ,
- adjusted determination coefficients  $R^2$ ,
- predicted determination coefficients  $R^2$ .

### Results and analysis for S1 – resin bond

Dependency between technological parameters for wheel with resin bond S1 as a function of temperature  $T$  and force  $F_n$  was shown in Figure 8.

Equations of mathematical models describing the changes in temperature  $T$  are presented below (Exp. 5) as well as the component  $F_n$  of the grinding force (Exp. 6) as a function of technological parameters.

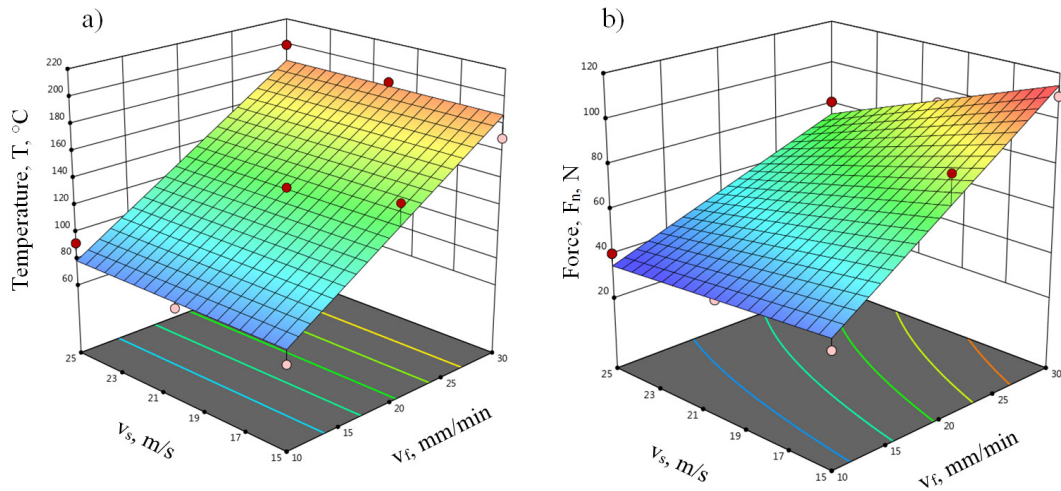


Fig. 8. Dependency between technological parameters ( $v_f, v_s$ ) as a function of: a) temperature T, b) force  $F_n$

$$T = 132.8 + 54.18 \cdot v_f \quad (5)$$

$$F_n = 66.81 - 11.83 \cdot v_s + 28.18 \cdot v_f - 7.94 \cdot v_s \cdot v_f \quad (6)$$

The statistical parameters for the model (5), (6) are presented in Table 5.

The  $F_n$  normal component of the grinding force was analyzed and it was noticed that depending on the experiment, the force  $F_n$  varies from 37 N to 110 N and the range of the value for all tests is as high as 73 N. The highest value of  $F_n$  was registered for the highest feed rate  $v_f$ . The cutting speed  $v_s$  increased with decreasing of the force  $F_n$ . From the obtained mathematical model – feed rate  $v_f$  and cutting speed  $v_s$  have effect on the increase of  $F_n$  force. According to the conducted analysis the feed rate  $v_f$  exhibits the greatest influence. Habrat et al. [22] registered the influence of technological parameters on the grinding force  $F_n$  as well. The recorded force was in the range of 73–245 N.

While analyzing the results it was noted that the T grinding temperature varies from 200 to 68 °C depending on the experiment, and the range of the values is equal to 132 °C. The highest T temperature

was registered for number 3 and 7 grinding sample where grinding burns occurred. According to the conducted analysis that only feed rate  $v_f$  influences the rise of grinding temperature. Yang et al. [17] recorded temperature during grinding using a thermocouple as well. Grochalski et al. [23] recorded temperature using a thermocouple, but in the turning process.

Dependency between technological parameters for wheel with resin bond S1 as a function of surface roughness  $S_a, S_z$  is shown in Figure 9.

The dependencies between roughness parameters  $S_a$  and  $S_z$ , and the technological parameters for the wheel with resin bond S1 are presented below:

$$S_a = 0.3816 + 0.0375 \cdot v_s + 0.0563 \cdot v_f - 0.0156 \cdot v_s \cdot v_f + 0.0332 \cdot v_s^2 \quad (7)$$

$$S_z = 3.2 + 0.499 \cdot v_s + 0.3208 \cdot v_f \quad (8)$$

The statistical parameters for the model (7), (8) are presented in Table 6.

Analyzing the parameters of flute surface roughness  $S_a$ , it was discovered that depending on the experiment, it varied between 0.309 to 0.49  $\mu\text{m}$ , and the range of the values for all the

Table 5. The Statistical parameters for the model (5), (6)

Parameter	T	$F_n$
Std. dev s, °C/N	12.6	7.97
Mean value y, °C/N	132.80	66.81
C.V., %	9.49	11.92
R2	0.932	0.938
Adjusted R2	0.924	0.908
Predicted R2	0.891	0.739

Table 6. The statistical parameters for the model (7), (8)

Parametr	$S_a$	$S_z$
Std. dev s, $\mu\text{m}$	0.0125	0.3492
Mean value y, $\mu\text{m}$	0.4015	3.20
C.V., %	3.11	10.89
R2	0.975	0.712
Adjusted R2	0.955	0.629
Predicted R2	0.849	0.261



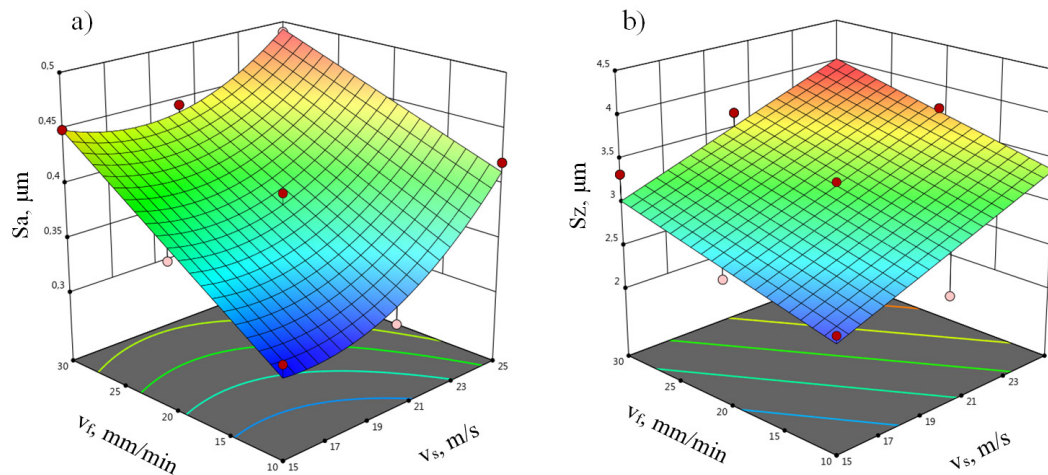


**Fig. 9.** Dependency between technological parameters ( $v_f, v_s$ ) as a function of: a)  $S_a$  roughness parameter, b)  $S_z$  roughness parameter

samples was as low as  $0.191 \mu\text{m}$ . According to the conducted analysis feed rate  $v_f$  and cutting speed  $v_s$  influence the surface roughness parameters. It was determined that technological parameters influence in statistically significant way the roughness parameters  $S_a$  and  $S_z$ , although the influence is low judging from the value's range.

### Results and analysis for S2 – metal bond

The dependency between technological parameters for wheel with metal bond S2 as a function of temperature  $T$  and force  $F_n$  is shown in Figure 10.

The equations of mathematical models describing the changes of temperature  $T$  are presented below (Exp. 9) as well as the component  $F_n$  of the grinding force (Exp. 10) as a function of technological parameters.

$$T = 63.74 - 7.73 \cdot v_s + 26.30 \cdot v_f - 10.92 \cdot v_s \cdot v_f \quad (9)$$

$$F_n = 52.22 - 14.77 \cdot v_s + 20.50 \cdot v_f - 10.91 \cdot v_s \cdot v_f \quad (10)$$

The statistical parameters for the model (9), (10) are presented in Table 7.

The  $F_n$  normal component of the grinding force was analyzed and it was noticed that depending on the experiment, the force varies from 28 to 90 N, and the range of the values for all tests was equal to 62 N. The highest force  $F_n$  was registered for

**Table 7.** The statistical parameters for the model (9), (10)

Parametr	T	$F_n$
Std. dev s, °C/N	6.06	9.10
Mean value y, °C/N	63.74	52.22
C.V., %	9.50	17.43
R2	0.957	0.896
Adjusted R2	0.936	0.844
Predicted R2	0.858	0.575

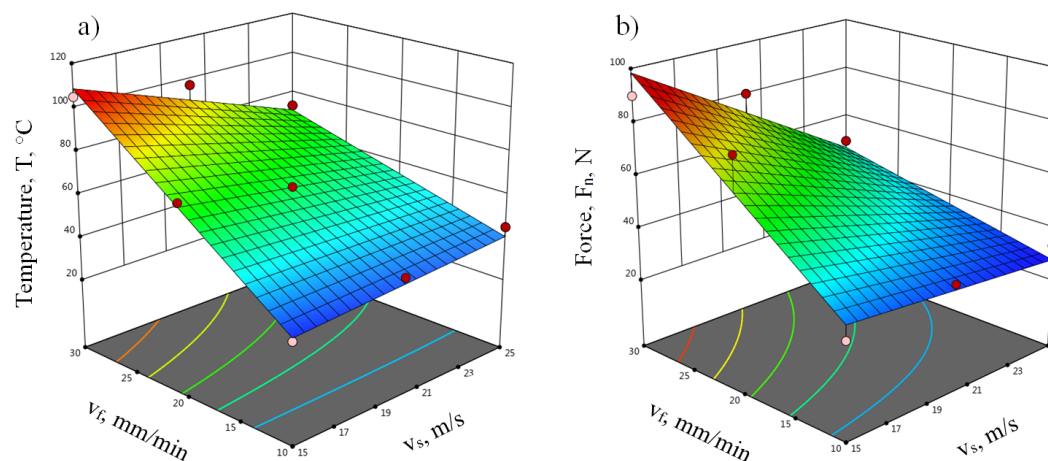


**Fig. 10.** Dependency between technological parameters ( $v_f, v_s$ ) as a function of: a) temperature  $T$ , b) force  $F_n$

the highest feed rate  $v_f$  and with increasing cutting speed  $v_s$ , a decrease of the force  $F_n$  was observed. According to the conducted analysis, feed rate  $v_f$  and cutting speed  $v_s$  influence the force  $F_n$ , but feed rate  $v_f$  shows the most significant influence. Habrat et al. [22] registered the influence of technological parameters on the grinding force  $F_n$  as well. The recorded force was in the range of 73–245 N.

While analyzing the results, it was noted that the grinding temperature  $T$  varied from 105 to 32 °C depending on the experiment and the range of the values was equal to 73 °C. The highest  $T$  temperature was registered for grinding sample number 1 and 7, where the highest value of speed rate  $v_f$  occurred. According to the conducted analysis, feed rate  $v_f$  and cutting speed  $v_s$  influence the rise of temperature  $T$ , but feed rate  $v_f$  shows the most significant influence. Yang et al. [17] recorded temperature during grinding using a thermocouple as well. Grochalski et al. [23] recorded temperature using a thermocouple, but in the turning process.

On the basis of the results it was not possible to develop mathematical models of  $S_a$  and  $S_z$  as a function of technological parameters. It follows from the fact that the range of the values for individual tests is only 0.140  $\mu\text{m}$ . Analyzing the parameter values of flute surface roughness  $S_a$ , it was discovered that depending on the experiment, it changes between 0.624 to 0.764  $\mu\text{m}$ . Abdullah et al. [21] registered slight influence of feed rate  $v_f$  and grinding speed  $v_s$  on the surface roughness as well. The recorded surface roughness was in the range of 0.25–0.4  $\mu\text{m}$ .

### Results and analysis for booth wheel (S1, S2) – summary

While examining the grinding temperature  $T$  and the two wheels with two different bonds (S1, S2), it can be noticed that wheel with metal bond (S2) generates lower grinding temperature  $T$  in comparison to wheel with resin bond (S1), which is shown in Figure 11. Average value of temperature for all the grinding passes (DoE) equals to 132 °C for the S1 wheel and to 63 °C for the S2 wheel. Usage of the wheel S2 lowers average value of flute temperature in single pass by 53%.

Analyzing the grinding force  $F_n$  and the two wheels with two different bonds (S1, S2), it can be noticed that wheel with metal bond (S2) generates lower grinding force  $F_n$  in comparison with the wheel with resin bond (S1), which is shown in Figure 12. Average value of the force  $F_n$  for all the passes (DoE) for the wheel S1 equals to 66 N, and for the wheel to S2–52 N. Usage of the wheel S2 lowers average value of flute temperature in single pass grinding by 21%.

Analyzing roughness parameters  $S_a$  and  $S_z$  and the two wheels with two different bonds (S1, S2), it can be noticed that the wheel with resin bond (S1) generated lower values of roughness parameters in comparison with the wheel with metal bond (S2) – Figure 13, 14. The average value of the  $S_a$  roughness parameter for all grinding passes (DoE) for the S1 grinding wheel was equal to 0.401  $\mu\text{m}$  and for the grinding wheel S2 to 0.688  $\mu\text{m}$ . The use of the S1 grinding wheel reduced the value of the  $S_a$  roughness of the flute on average by 41%.

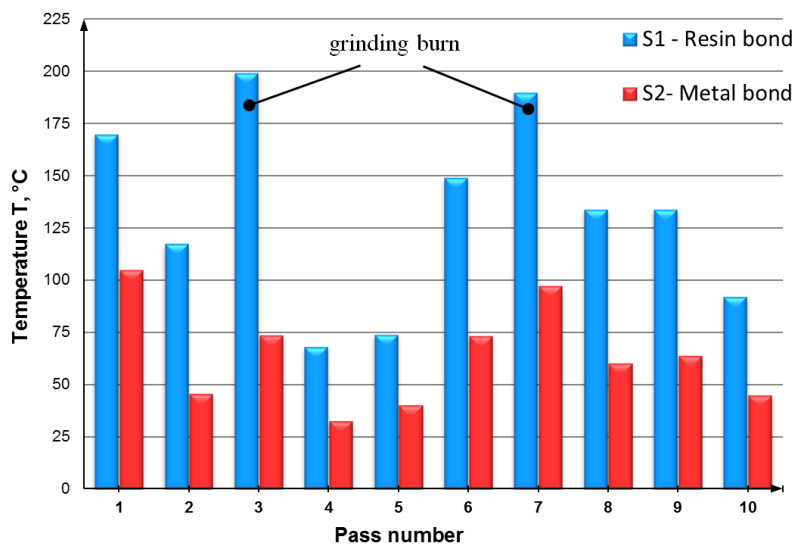


Fig. 11. The results of the temperature  $T$  measurement for both wheels

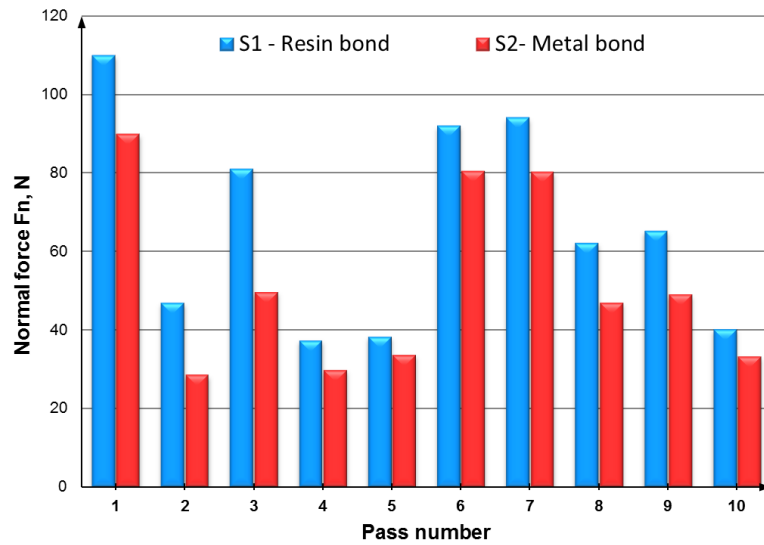


Fig. 12. The results of the normal force  $F_n$  measurement for both wheels

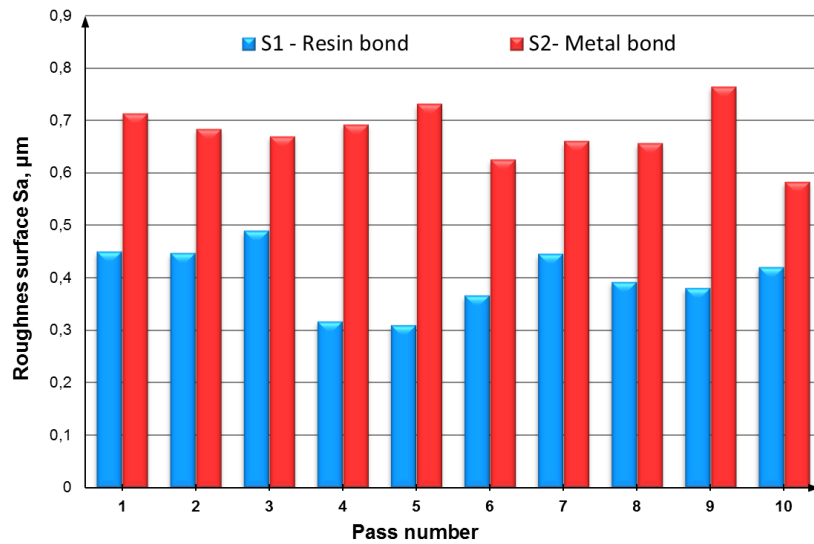


Fig. 13. The results of the roughness surface  $S_a$  measurement for both wheels

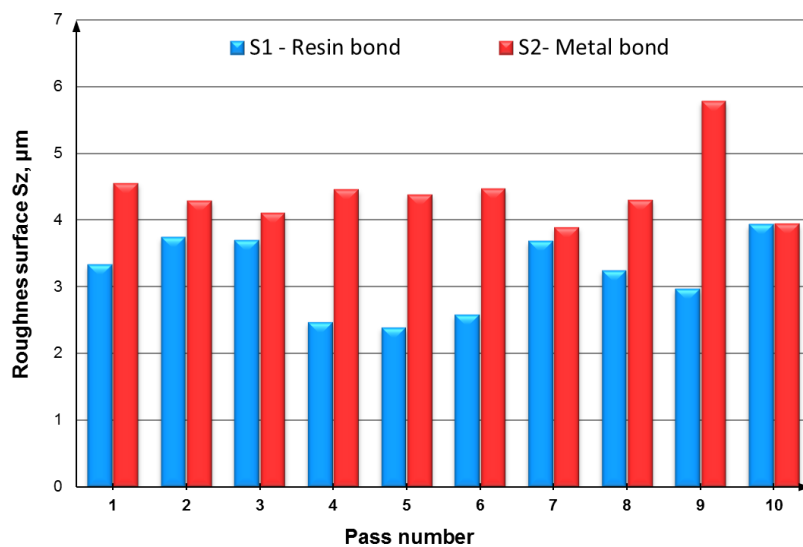


Fig. 14. The results of the roughness surface  $S_z$  measurement for both wheels

The average value of the Sz roughness parameter for all the passes (DoE) for the S1 wheel was equal to 3.20  $\mu\text{m}$  and for the S2 grinding wheel to 4.42  $\mu\text{m}$ . The use of the S1 grinding wheel reduced the value of the Sz roughness of the flute on average by 27%.

## CONCLUSIONS

Thanks to the designed measuring stand it was possible to register not only grinding force  $F_n$  but also grinding temperature T which is a significant aspect. Measurement of grinding force normal component  $F_n$  is also crucial, as value of the force influences the elastic displacements of the tool. High values of the elastic displacements lead to dimensional errors of grinded end mills. As the experiments has shown, the measurement of temperature in the grinding process indicates the occurrence of grinding burns. It is a key information concerning correct single pass flute grinding process of a TSF44 carbide.

Grinding burns were observed during the experiment, although they were classified as “light ones”—which enabled further experiments. Outside of the assumed design of experiment, for parameters  $v_s = 25$  m/s,  $v_f = 30$  mm/min,  $a_e = 3.5$  mm  $a_p = 4.77$  mm “strong” grinding burns were observed, which did not allow to continue further experiments. Measured temperature value was equal to 485 °C.

The grinding efficiency  $Q_w$  in carried out researches varied from 100 to 301 mm<sup>3</sup>/mm. For the S1 wheel, for grinding pass number 3 and 7 (in which the grinding efficiency was the highest  $Q_w = 301$ ) with the feed rate  $v_f = 30$  mm/min, grinding burns were observed. For grinding pass number 1, where feed rate  $v_f$  was also 30 mm/min the grinding burn was not observed, what results from using the smallest grinding speed  $v_f = 15$  m/s.

It should be mentioned that the flute in solid carbide end mills is responsible for the evacuation of the chip from the machining zone. Therefore, the roughness of the flute is the key to proper chip evacuation. In addition to the roughness parameters, an important factor in assessing the quality of the flute surface is the presence of defects in the form of scratches or inclusions. No surface heterogeneity or irregular inclusions were observed in any grinding test.

The developed mathematical models for different technological parameters ( $v_p$ ,  $v_s$ ) as a function

of T,  $F_n$ , Sa, Sz can help to optimize the grinding process. The correlation between the temperature T and the grinding parameters ( $v_p$ ,  $v_s$ ) allows to determine the non-recommended parameters, which allows to avoid grinding burns, thus extending the grinding wheel time. The correlation between the grinding force  $F_n$  and the grinding parameters ( $v_p$ ,  $v_s$ ) allows to reject grinding parameters, for which the dimensional errors of grinded end mills would be the highest ( $F_n = \text{max}$ ).

## REFERENCES

1. Malkin S., Guo C. Grinding Technology: Theory and Application of Machining with Abrasives. Industrial Press; 2008.
2. Hubert Ch. Schleifen von Hartmetall- und Vollkeramik – Schaftfräsern. Berlin: TU, Diss.; 2011.
3. Fujara M. Methode zur rechnerunterstützten Auslegung und Optimierung der Geometrie des Vollhartmetall-Spiralbohrers. Darmstadt: Techn. Univ., Diss.; 2011.
4. Christoph H. Schleifen von Hartmetall- und Vollkeramik Schaftfräsern. Berlin: TU, Diss.; 2011.
5. Guachao L., Lie S., Jiafeng L. Modeling and analysis of helical groove grinding in end mill machining. Journal of Materials Processing Technology. 2014; 214(12): 3067–3076.
6. Burek J., Sałata M., Bazan A. Influence of grinding parameters, on the surface quality in the process of single-pass grinding of flute in solid carbide end mill. Mechanik. 2018; 91(10): 808–810.
7. Burek J., Sałata M., Bazan A. The influence of the type of grinding wheels bond on flute grinding of carbide tools. Mechanik. 2016; 91(8–9): 1130–1131.
8. Yang J., Odén M., Johansson-Jöesaar M.P., Llanes L. Grinding effects on surface integrity and mechanical strength of WC-Co cemented carbides. In: Proc. of 2nd CIRP Conference on Surface Integrity (CSI), Nottingham, UK 2014, 257–263.
9. Uhlmann E., Hübert C. Tool grinding of end mill cutting tools made from high performance ceramics and cemented carbides. CIRP Annals - Manufacturing Technology. 2011; 60(1): 359–362.
10. Badger J. Grinding of sub-micron-grade carbide: Contact and wear mechanisms, loading, conditioning, scrubbing and resin-bond degradation. CIRP Annals - Manufacturing Technology. 2015; 64(1): 341–344.
11. Bazan A., Kawalec A., Rydzak T., Kubik P. Variation of Grain Height Characteristics of Electroplated cBN Grinding-Wheel Active Surfaces Associated with Their Wear. Metals. 2020; 10(11): 1479.



12. Bazan A., Kawalec A., Rydzak T., Kubik P., Olko A. Determination of Selected Texture Features on a Single-Layer Grinding Wheel Active Surface for Tracking Their Changes as a Result of Wear. *Materials*. 2021; 14(1): 6.
13. Ren Y.H., Zhang B., Zhou Z.X. Specific energy in grinding of tungsten carbides of various grain sizes. *CIRP Annals - Manufacturing Technology*. 2009; 58(1): 299–302.
14. Shatov A.V., Ponomarev S.S., Firstov S.A. Hardness and Deformation of Hardmetals at Room Temperature. *Comprehensive Hard Materials*. 2014; 1: 267–299.
15. Sui M., Li C., Wu W., Yang M., Ali H.M., Zhang Y., Cao H. Temperature of grinding carbide with castor oil-based MoS<sub>2</sub> nanofluid minimum quantity lubrication. *Journal of Thermal Science and Engineering Applications*. 2021; 13(5): 051001.
16. Ren X., Huang X., Chai Z., Li L., Chen H., He Y., Chen X. A study of dynamic energy partition in belt grinding based on grinding effects and temperature dependent mechanical properties. *Journal of Materials Processing Technology*. 2021; 294: 117112.
17. Yang M., Li C., Luo L., Li R., Long Y. Predictive model of convective heat transfer coefficient in bone micro-grinding using nanofluid aerosol cooling. *International Communications in Heat and Mass Transfer*. 2021; 107: 2411–2502.
18. Bazan A., Kawalec A., Babiarz R., Krupa K. Temperature measurement using natural thermocouple during grinding with monolayer grinding wheel. *Mechanik*. 2017; 90(8–9): 760–762.
19. Grochalski K., Jabłoński P. Comparison contact and thermal imaging methods measure the temperatures of the turning blades during cutting. *Mechanik*. 2017; 90(3): 214–216.
20. Ren L., Wang S., Yi L., Sun S. An accurate method for five-axis flute grinding in cylindrical end-mills using standard 1V1/1A1 grinding wheels. *Precision Engineering*. 2016; 43: 387–394.
21. Abdullah A., Pak A., Farahi M., Barzegari M. Profile wear of resin-bonded nickel-coated diamond wheel and roughness in creep-feed grinding of cemented tungsten carbide. *Journal of Materials Processing Technology*. 2007; 183(2): 165–168.
22. Habrat W.F. Effect of bond type and process parameters on grinding force components in grinding of cemented carbide. *Procedia Engineering*. 2016; 149: 122–129.
23. Grochalski K., Jabłoński P., Talar R., et al. Temperature Measurement of Modern Cutting Tools During Turning. *Advances in Science and Technology Research Journal*. 2020; 14(4): 37–48.
24. Burek J., Babiarz R., Sałata M., Krok M. Force measurement during carbide end mill grinding. *Mechanik*. 2016; 11: 1738–1739.
25. EN ISO 25178-2:2012 Geometrical product specifications (GPS) – Surface texture: Areal-Part2: Terms, definitions and surface texture parameters.
26. National Instruments. Ni USB-621x User manual. June 2021
27. <https://www.guenther.com.pl/en/>. June 2021
28. Habrat W., Żółkoś M., Świder J., Socha E. Forces modeling in a surface peripheral grinding process with the use of various design of experiment (DoE). *Mechanik*. 2018; 10: 929–931.
29. Krajnik P., Kopač J. Adequacy of matrix experiment in grinding. *Journal of Materials Processing Technology*. 2004: 566–572.
30. Montgomery D.C. *Design and Analysis of Experiments*. Hoboken, NJ: John Wiley & Sons; 2017.
31. *Handbook for Experimenters*- version 13. Inc. Minneapolis USA; 2021
32. Markopoulos A.P., Habrat W., Galanis N.I., Karkalos N.E. *Modelling and Optimization of Machining with the Use of Statistical Methods and Soft Computing. Design of Experiments in Production Engineering*. Switzerland: Springer International Publishing; 2016.